μ-Synthesis Based, Robust Controller Design for AMB Machining Spindles

L. Scott Stephens, Assistant Professor
2508 CEBA, Louisiana State University,
Department of Mechanical Engineering, Baton Rouge, LA
Tel : (504)388-5905; Fax : (504)388-5924; e-mail: stephens@me.lsu.edu

Carl R. Knospe, Assistant Professor
University of Virginia, School of Engineering & Applied Sciences,
Department of Mechanical, Aerospace and Nuclear Engineering, Charlottesville, Virginia,22908
Tel : (804)982-2603; e-mail: carl@romac1.mech.virginia.edu

Abstract: Due to high surface speed and active control capabilities, active magnetic bearings (AMB's) have found a niche in high speed machining spindle applications. This paper presents a formulation of the μ-synthesis based robust controller design problem for AMB machining spindles which uses specifications based upon cutting performances such as profiling, surface finishing and rough cutting accuracy. A new method for casting the machining chatter rejection tendency in terms of a μ based performance specification is presented. With this tool, controllers can be designed such that this tendency can be minimized. The formulation also includes uncertainty representing a range of cutting tools for the spindle and the AMB's. Synthesis results indicate that this formulation is effective in achieving robust cutting and chatter rejection performance.

1 Introduction

Figure 1 shows a schematic of an AMB machining spindle consisting of three radial magnetic bearings, termed the *nose, mid-span,* and *tail bearings*. The shaft is dual level with a large rotor on which all bearing journals and the motor rotor are carried, and a smaller drawbar located within an internal bore of the main rotor. The purpose of the drawbar is to actuate the cutting tool, allowing for tool changes, as several different tools may be used during a machining operation. The cutting force applied at the tool tip is also shown. The objective is to control the flexible shaft such that motion at the cutting tool tip is minimized. The challenge for machining is the complex nature of the cutting force and process dynamics.

Previous work in robust control of flexible shafts using AMB's has shown promising results. Nonami and Ito[5] described centralized 5-axis μ-synthesized controller design using a rigid body rotor model of a flexible rotor magnetic bearing system. Fujita[3] presented experimental results for μ-synthesized controllers suspending a non-rotating beam in magnetic bearings. In both works, experimental results showed superior performance of the μ-synthesized controllers over H_∞ loop shaping and PID controllers. The performance was based on robust low frequency output disturbance rejection in the presence of input multiplicative or additive uncertainty. Formulation of the μ-synthesis problem in this manner is sufficient for a broad class of applications, however, characterization of machining spindle performance in cutting processes is significantly more complex. This paper presents a new formulation of the problem which is motivated by the cutting operation.

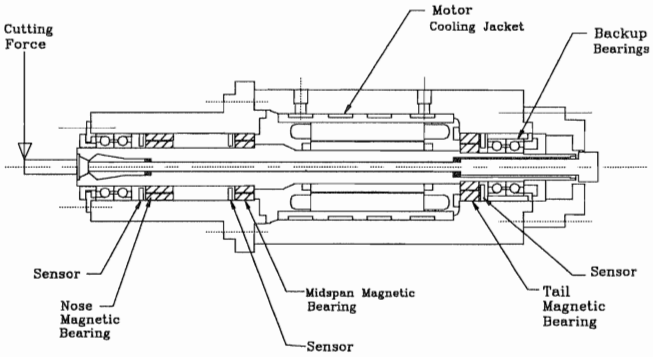

Figure 1: AMB Machining Spindle

2 Robust Control

The basis of robust control is accurately modeling system uncertainty using perturbations on the nominal model, and synthesizing controllers which perform in spite of the uncertainty. Complex perturbations, denoted $\Delta(j\omega)$, are norm-bounded using the transfer function ∞-norm,

$$\|\Delta(j\omega)\|_\infty = \sup_\omega \bar{\sigma}[\Delta(j\omega)] \qquad (1)$$

and are normalized by stable minimum phase frequency dependent weighting functions $W(j\omega)$, which are appended to the system model such that $\|\Delta\|_\infty \le 1$ represents the range of uncertainty in the system dynamics. Similarly, real parameter perturbations, denoted δ, are norm-bounded and normalized by constant weights, a, such that $\|\delta\|_\infty \le 1$ represents the range of uncertainty in real parameters.

Perturbation locations are preserved during controller design and analysis by using the *structured singular value*, μ, as a measure of the closed loop stability and performance. The structured singular value of closed loop system $M \in C^{nxn}$, for complex perturbations $\Delta \in C^{nxn}$, is defined as:

$$\mu(M) := \frac{1}{\min\left(\bar{\sigma}(\Delta) : \det(I - M\Delta) = 0\right)} \tag{2}$$

where Δ is a member of the block diagonal set $\underline{\Delta}$. Computation of the structured singular value using equation 2 is intractable, but bounds on μ can be computed for complex perturbations using the following well-known relations [1]:

$$\max_{\Gamma \in \underline{\Gamma}} \rho(\Gamma M) \le \mu(M) \le \inf_{D \in \underline{D}} (\bar{\sigma})(DMD^{-1}) \tag{3}$$

where, among others, D is any real, diagonal, positive matrix with a certain block diagonal structure. Computation of μ for mixed complex/real perturbations is accomplished using a similar set of equations [2].

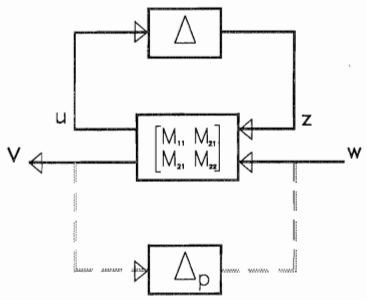

Figure 2: General LFT Representation

μ finds it's usefulness as the basis for a set of stability and performance tests for uncertain systems. Consider Figure 2, where M is the nominal closed loop system model with all performance and uncertainty weights included, Δ represents plant uncertainty and Δ_p represents plant performance, where $\Delta_p \in \underline{\Delta}$. The relationship between the performance inputs, v, and outputs, w, is determined by the upper LFT on the block matrix M, and leads to the following stability and performance tests:

$$\mu_\Delta(M_{22}) < 1 \qquad \textit{Nominal Performance} \tag{4}$$

$$\mu_\Delta(M_{11}) < 1 \qquad \textit{Robust Stability} \tag{5}$$

$$\mu_\Delta(M) < 1 \qquad \textit{Robust Performance} \tag{6}$$

where nominal performance is specified performance of the nominal plant, robust stability is stability of all uncertain plants, and robust performance is specified performance of all uncertain plants. Note that if robust performance is satisfied, then nominal performance and robust stability are implied as well.

Design of controllers in a μ framework is accomplished using the DK iteration method. Since the upper bound for μ in equation 3 may be obtained by scaling and applying $\|\cdot\|_\infty$, DK iteration proceeds by finding a stabilizing H_∞ controller, K, and a scaling matrix, D, such that the following minimization occurs:

$$\min_{D \in \underline{D}, K} \left\| DF_l(P,K)D^{-1} \right\|_\infty \tag{7}$$

where $F_l(P,K)$ is the lower LFT between the open loop system, P, and the stabilizing controller, K [2].

3 System Modeling

The nominal model consists of the AMB actuators, spindle dynamics, sensors, filters, digital controller, amplifiers and a cutting force description. The linearized force expression for the AMB's in each orthogonal direction, x_i, i=1,2, is given by the following equation:

$$F_i = \frac{-4\mu_0 AN^2 I_b^2}{g^3} x_i + \frac{4\cos\left(\frac{\pi}{8}\right)\mu_0 AN^2 I_b}{g^2} I_{p,i} \tag{8}$$

where N is the number of turns in each coil, A is the cross sectional area of each pole and g is the radial air gap. A planar, dual level rotordynamic model of the spindle and drawbar is used.

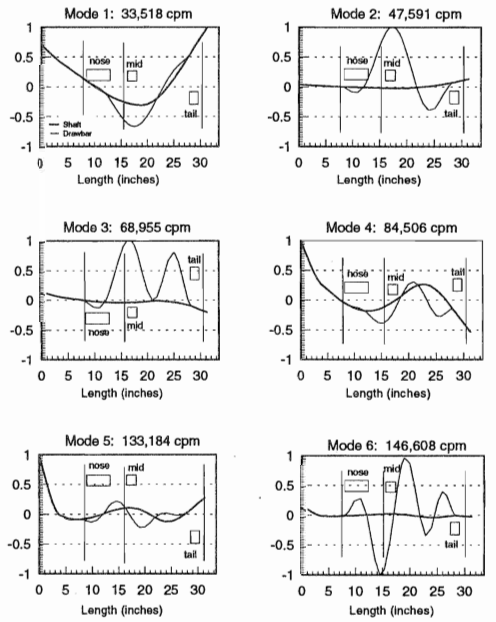

Figure 3: Free-Free Rotordynamic Modes

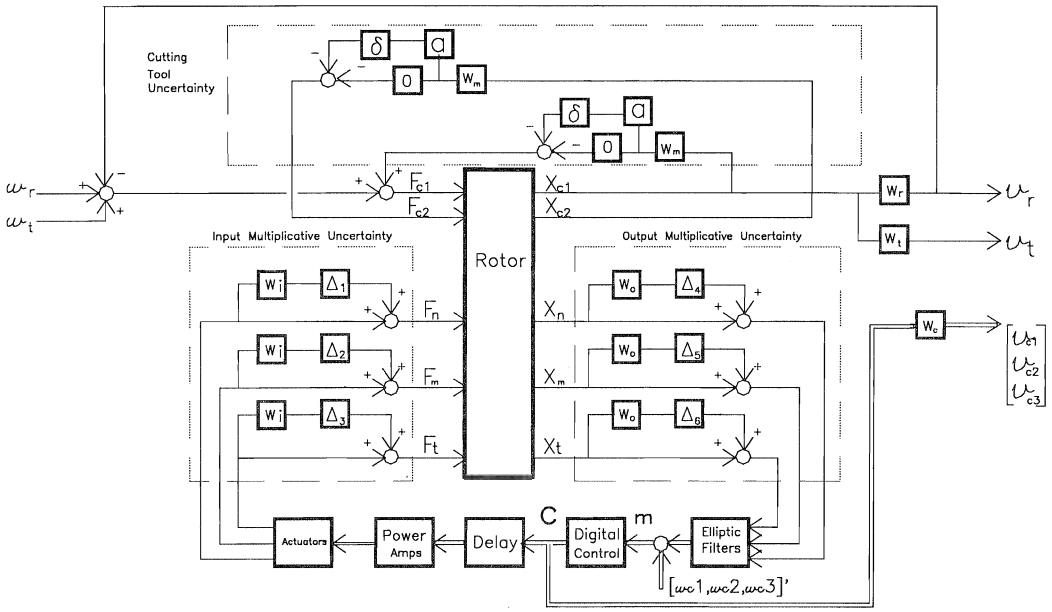

Figure 4: AMB Machining Spindle Model

The housing is assumed rigid and gyroscopic effects are negligible. The first six free-free critical speeds and modeshapes of the rotor and drawbar model including bearing and motor negative stiffness are shown in Figure 3. The first four modes are within the controller bandwidth. Modal damping of 1 % is included, and the bearing actuator and sensor locations are also shown.

Sensors are modeled as a unity gain with noise, and low pass Cauer filters are used to suppress the noise. Pure phase lag is used to approximate the zero order hold and throughput delay of a digital controller. Power amplifiers are modeled using a first order approximate transfer function as given below.

$$G_{amps} = \frac{18600}{s+6200} \tag{9}$$

The cutting force magnitude depends upon many factors which are specific to the machine tool and type of cut. Description of such factors is beyond the scope of this design. However, for the process of end milling of aluminum alloys, the predominant frequency content of the cutting force consists of harmonics of the cutting tooth frequency, f_{ct}, a forced vibration, and machining chatter frequency, f_c, a self excited vibration [7].

With this characterization of the cutting force spectrum, the following objectives with regard to controller design are formulated: (i) reduce the tool harmonic response at multiples of the toothpass frequency, f_{ct}, and, (ii) suppress the onset of machining chatter which occurs at chatter frequency, f_c. Machining chatter, which occurs at different combinations of running speed and axial width of cut, can be characterized by a limiting axial width of cut for stable machining at all speeds. This asymptotic stability borderline is given as [8]:

$$b = -\frac{1}{2K_s Re[G]} \tag{10}$$

where b is the axial width of cut at the limit of stability, K_s is the cutting stiffness of the workpiece material and $Re[G]$ is the real part of the oriented transfer function of the system. In the absence of a specific cutting process, chatter then occurs at the most negative real part of the dynamic compliance of the spindle at the cutting tool. Therefore, in order to satisfy objective (ii) listed above, the minimum *real tip compliance* of the spindle should be maximized.

Figure 4 shows a model of the nominal system with all uncertainties and performance weights. The most significant uncertainty in the feedback loop enters into the system at the AMB actuators as the actuator nominal model does not include hysteresis, eddy currents, large deflections nor leakage or fringing effects.

The feedback loop uncertainties are encompassed in a single guaranteed multivariable stability margin specification [6] at either the plant input, which represents actuator uncertainty, or the plant output which represents measurement uncertainty. The multiplicative uncertainties, $\Delta_1 - \Delta_6$, are complex, and the weights, W_i=0.2 and W_o=0.2, correspond to a guaranteed multivariable gain margin of ±20% .

Significant uncertainties occur in the modeling of the spindle rotordynamics because different cutting tools are utilized for different cutting operations by the machining spindle. The mass of possible cutting tools ranges between 0.00138 and 0.0034 lb.s^2/in. Due to this variation, the first natural frequency of the system varies between 29,254 CPM and 34,890 CPM over the range of cutting tools.

The location of the cutting tool mass uncertainty, δ, in the machining spindle model is also shown in Figure 4. The tool mass is distributed in reality, therefore lumped mass is fedback at two locations along the length of the nominal cutting tool to approximate this condition. The tool mass uncertainty weights consist of two parts; W_m, which is a rational transfer function and approximates a second order polynomial over the frequency range of interest, and a, the tool mass parameter, which represents a real parameter variation. The rational transfer function used is given in the following equation.

$$W_m = 2.35e^8 \frac{(s+100)(s+200)}{(s+10{,}000)(s+11{,}000)} \tag{11}$$

The tool mass variation is taken as half the mass of the largest tool, such that a=0.0017 ($lbf \cdot s^2 / in$).

4 Performance Specifications

Referring once again to Figure 4, the performance weights W_b, W_r and W_c which limit direct tip compliance, real tip compliance and controller effort, respectively, are shown. The performance inputs are shown as $\mathbf{w}=[w_n, w_b, w_{c1}, w_{c2}, w_{c3}]'$ and the performance outputs are shown as $\mathbf{v}=[v_n, v_b, v_{c1}, v_{c2}, v_{c3}]'$. Also shown are the bearing forces, F_n, F_m, F_t, and the shaft displacements, X_n, X_m, X_t at the nose, midspan and tail sensors respectively. Finally, inputs F_{c1} and F_{c2} represent applied forces at the cutting tool tip and tool midspan, and outputs X_{c1} and X_{c2} represent the displacement at the cutting tool tip and tool midspan, respectively.

Compliance of the spindle at the cutting tool tip is an indicator of how the spindle may perform in certain cutting operations. For instance, static tip compliance, G_{dc}, indicates the positioning accuracy of the tool tip, and low frequency tip compliance, G_{lf}, indicates the profiling accuracy of the spindle. The latter frequency range is determined by considering the maximum acceleration of the spindle by the machine tool in which it is mounted, and the radius of curvature of possible profiles that may be cut with the spindle. The limit on acceleration is 0.5-1.0 g's in typical spindles, therefore the low frequency range is taken as 50-400 rad/s which corresponds to cut radii as low as 0.002 in.

The medium frequency tip compliance, G_{mf} indicates the rough cutting performance of the spindle. The medium frequency range is taken as the toothpass frequency range corresponding to the spindle operating speed.

Finally, the high frequency tip compliance, G_{hf}, indicates the performance of the spindle in finishing cuts. This range is taken as 10,000-100,000 rad/s. All four tip compliance frequency ranges are encompassed in a single performance specification, Wt, given by the following transfer function:

$$W_t = \frac{s+50}{6E^{-5}(s+10)} \tag{12}$$

which allows a static compliance of $12.3E^{-6}$ in/lbf, and a dynamic compliance of 5 times the static.

A performance weight requiring minimum control effort provides for the maximum allowable cutting force and sensor noise. The control effort performance weight is given by the following transfer function.

$$W_c = \frac{s+4000}{20000(s+32000)} \tag{13}$$

This specification is applied only to the *direct* control effort, not the cross-coupled terms in the MIMO controllers.

As previously shown, the minimum real tip compliance, G_{re}, is an index of the tendency of the spindle to chatter and therefore must be maximized. Incorporation of this criterion as a performance specification requires a different formulation than the previous criterion. A real tip compliance specification requires a negative unity feedback loop around the tip compliance transfer function, G_c. Figure 5 illustrates such a block below and leads to the following theorems [4].

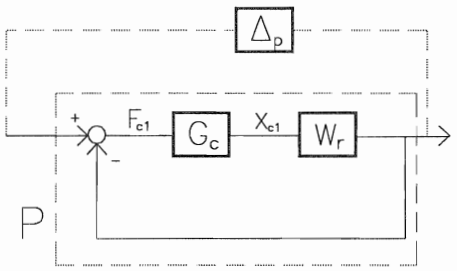

Figure 5: Real Tip Compliance Performance Block

Theorem 1: *If* $\|P\|_\infty < 1$ *then:*

$$\mathrm{Re}[G_c] > -\frac{1}{2W_r} \tag{14}$$

Proof: At a particular frequency $G_c(j\omega) = a + bj$, where a and b are the real and imaginary parts of G_c, and the condition $\|P\|_\infty < 1$ requires:

$$\left|\frac{G_c W_r}{1+G_c W_r}\right| < 1 \tag{15}$$

or

$$\left|\frac{(a+bj)W_r}{1+(a+bj)W_r}\right| < 1 \tag{16}$$

converting this equation to the squared magnitude yields:

$$(aW_r)^2 - (bW_r)^2 < (1+aW_r)^2 - (bW_r)^2 \tag{17}$$

which simplifies to:

$$a > -\frac{1}{2W_r} \tag{18}$$

for $W_r > 0$.

Theorem 2: *If* $\|P\|_\infty < 1$ *then the major feedback loop in Figure 5 is stable.*

Proof: By definition $\|\Delta_p\|_\infty < 1$. Therefore, by the small gain theorem, Theorem 2 holds.

Theorem 1 provides the means of specifying the minimum real tip compliance, while Theorem 2 provides a means of casting this specification in a μ framework such that DK iteration will work to achieve it. One caveat must be mentioned when using this method: the minor feedback loop must be stable. This is guaranteed by the small gain theorem if $\|G_c W_r\|_\infty < 1$, which implies that $\|G_c\|_\infty < W_r^{-1}$ is sufficient. Figure 6 illustrates the requirement upon the tip dynamic compliance, G_c, in the complex gain plane for specification of real dynamic compliance.

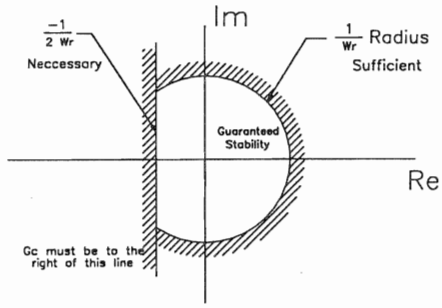

Figure 6: Requirement On Dynamic Compliance for Specification Of Real Dynamic Compliance

Typically, values of the dynamic compliance, G_c, are relatively small. Therefore stability of the minor loop is likely. For the spindle, the real tip compliance weight is taken as W_r = 15000, which corresponds to a minimum real tip compliance of $Re[Gc] > -3.33e^{-5}$ *in/lbf.* This specification is motivated quite arbitrarily by using the resulting minimum real tip compliance from nominal performance of the system under PD control as a benchmark.

5 Results

Four different controllers, K_1 - K_4, were designed using different combinations of the performance and uncertainty weights. The system was evaluated for each of the controllers using the robust performance test of equation 6 relative to only those performance specifications and uncertainties used for the controller design. Robust and nominal performance of the system with each controller is summarized in Table 1, including μ_{max} and the resulting controller order. Note that the plant order for this system is 58, compared to controller orders of about 100. Of course, for experimental implementation the order of such controllers should be reduced.

Table 1: Performance With Design Weights:

$W_1 = \frac{s+50}{6e^{-5}(s+10)}$, $W_2 = \frac{s+4000}{20000(s+32000)}$, $W_3 = \frac{1}{5e^{-2}}$, $W_4 = \frac{1}{2e^{5}}$,

$W_5 = 2.35e^{8}\frac{(s+100)(s+200)}{(s+10000)(s+20000)}$

Controller				K_1	K_2	K_3	K_4
Order				102	104	104	78
Performance			μ_{max}	0.61	0.58	1.112	0.99
	Robust	Des Wts	W_t	W_1	W_1	W_1	W_3
			W_r	–	–	15000	–
			W_c	W_2	W_2	W_2	W_4
			W_o	0.2	–	0.2	–
			W_i	–	0.2	–	–
			W_m	–	–	–	W_5
			a $(\frac{lbf \cdot s^2}{in})$	–	–	–	0.0017
	Nominal		G_{dc} $(\frac{\mu in}{lbf})$	0.7	0.8	6.0	1120.1
			G_{tf} $(\frac{\mu in}{lbf})$	2.6	2.9	8.4	1120.1
			G_{mf} $(\frac{\mu in}{lbf})$	18.4	23.5	25.7	58.3
			G_{hf} $(\frac{\mu in}{lbf})$	18.4	23.5	24.3	4.3
			G_{re} $(\frac{\mu in}{lbf})$	-9.6	-9.3	-8.2	-187.0
			$\frac{G_{dc}}{d_t}$	0.15	0.17	1.23	162.3

5.1 Robust Performance

Controller K_1 is designed to satisfy the maximum tip compliance specification, W_t, using the minimum control effort, W_c, for all uncertain plants represented by an output multiplicative uncertainty, W_o. Controller K_1 gives the worst case direct tip compliance indicating cutting performance, notwithstanding chatter, for a spindle operating with the nominal cutting tool using the specified amount of control effort. Robust performance results as μ_{max}= 0.61 for this case.

Controller K_2 is designed for the same weights as in K_1 except the feedback loop uncertainty is at the plant input, W_i. Very little difference in robust performance is seen between uncertainty at the output or at the input of the plant as μ_{max} = 0.58 for this case.

Controller K_3 is designed for the same weights as in K_1 except that the specification on *real* tip compliance, W_r, is used to improve the chatter rejection tendency of the spindle. Again, this is done only for the nominal tool. Results for G_{re} in Table 1 show that using the real tip compliance performance specification results in a 15 % improvement in chatter rejection nominal performance of the spindle over the other cases. This illustrates the success of the minimum real tip compliance performance specification as formulated in section 5. Note that $\mu = 1.12$ for this case, indicating the difficulty in achieving both direct tip compliance and real tip compliance minimization simultaneously for all uncertain plants.

Finally, controller K_4 is designed to accommodate variations in tool mass, W_m. This controller design reveals the level of guaranteed performance over the range of all cutting tools that can be obtained. Note for this case the performance and

uncertainty weights must be significantly less restrictive than in previous cases in order to satisfy the robust performance test condition.

The results indicate good cutting performance and chatter rejection tendency for the system with the nominal tool and uncertainty in the feedback loop. However very poor performance results when significantly different tools are used for the same controller. This indicates that a different controller for each range of tools should be used.

5.2 Nominal Performance

Nominal performance of the static, low frequency, medium frequency, high frequency, and minimum real compliance at the tool tip is also given in Table 1. Smaller compliance magnitudes indicate better cutting performance for each of the frequency ranges.

For a means of comparison, the ratio of static compliance of the nominal cutting tool as mounted in the spindle to the static compliance of the nominal cutting tool if it were cantilevered is given as G_{dc}/G_t, where $G_t = 4.9\ \mu$ in/lbf. Note that for controllers K_1 and K_2 this ratio is less than unity indicating a better static compliance for the cutting tool when supported by the spindle than when simply cantilevered; but how can this be?

This phenomenon occurs because the μ synthesized control actually *lifts* the shaft at all bearing locations to meet the performance specifications. This is illustrated in Figure 7 where a typical PD control solution, which attempts to center the spindle at the bearings, is shown for comparison.

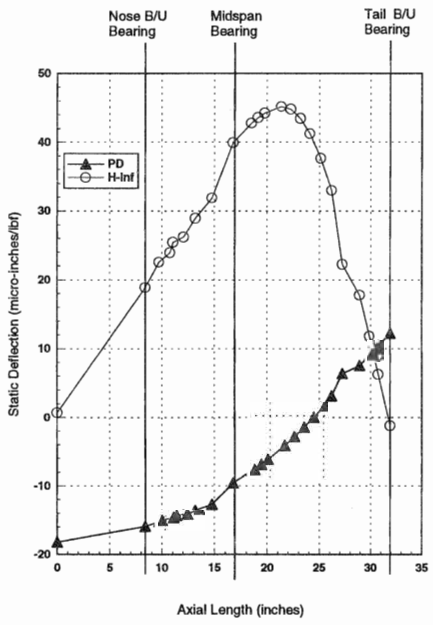

Figure 7: Static Deflection Profiles

Figure 7 indicates that a significant amount of deflection could occur at the backup bearings and midspan bearing due to the lifting. If the spindle is lifted too much, then a loss of bearing stability is likely to occur. Thus an additional set of performance specifications, which limit shaft displacement at critical locations along the shaft, should be included during controller synthesis.

6 Conclusions

The following conclusions can be offered from the above work: (1) μ-synthesized control can be used effectively to design for improved cutting performance of AMB spindles; (2) the chatter tendency of the spindle can be minimized using a performance block such that the minimum real part of the dynamic tip compliance is maximized; (3) only a small difference in performance occurs if feedback loop uncertainty is correctly modeled at the plant input as compared to the plant output; (4) when a large range of cutting tools are used in machining, very poor performance may result if the same controller is used for all tools; (5) a performance specification which limits shaft deflection at locations along the shaft with small clearances is required in this formulation.

References

[1] Doyle, J., "Analysis of Feedback Systems with Structured Uncertainties", *IEE Proceedings*, v. 120, part D, n. 6, November 1982, pp.242-250

[2] Doyle, J.C., "Structured Uncertainty in Control System Design", *Proceedings of 24th Conference on Decision and Control*, Ft. Lauderdale, FL, December, 1985, pp. 260-267

[3] Fujita, M., et. al., "μ Analysis and Synthesis of a Flexible Beam Magnetic Suspension System", *Proceedings of the Third International Symposium on Magnetic Bearings*, Alexandria, VA, July 29-31, 1992, pp.495-504

[4] Knospe, C.R., "Notes on Real Tip Compliance Performance", University of Virginia, 1995

[5] Nonami, K., and Ito, T., "μ-Synthesis of Flexible Rotor Magnetic Bearing Systems", *Proceedings of the Fourth International Symposium on Magnetic Bearings,* Zurich, Switzerland, August 25-28, 1994 fourth, pp. 73-78

[6] Safanov, M.G., "Stability Margins of Diagonally Perturbed Multivariable Feedback Systems", *IEE Proceedings*, Part D, pp. 251-256, November 1982

[7] Smith, S., and Tlusty, J., "Update on High Speed Milling Dynamics", *ASME Journal of Engineering for Industry*, v. 112, May 1990, pp. 142-149

[8] Tlusty, J., and Polacek, M., "Beispiele der Behandlung der selbsterregten Schwingung der Werkzeugmaschinen", 3. FoKoMa, Vogel-Verlag Wuerzburg, October, 1957.